Journal of
MARINE RESEARCH

Volume 35, Number 3

# Observations of the power and directional spectrum of ocean surface waves

by Lloyd A. Regier[1] and Russ E. Davis[2]

## ABSTRACT

Estimates of the power spectrum and directional spectrum of oceanic surface waves were obtained from data taken during the Barbados Oceanographic and Meteorological Experiment (BOMEX). Wind speeds ranged from 5 to 10 m $s^{-1}$ throughout the month's duration of the experiment.

The power spectra coalesce into a characteristic form when plotted against nondimensional frequency $\hat{f} = f/f_m$, where $f_m$ is the frequency of the power spectrum peak; the more conventionally used ratio of wind speed to wave phase speed was found not to be an appropriate frequency parameter. The characteristic power spectrum is inconsistent with the theoretical Phillips spectrum and the Pierson-Moskowitz empirical model. The power law relating the spectrum to $\hat{f}$ appears to change near $\hat{f} = 3$.

At a fixed frequency, $f < 3f_m$, the width of the directional spectrum increases when $f_m$ decreases and narrows as wind speed increases. The directional spectrum is quite variable, indicating that propagation of energy from distant areas is important at all frequencies up to .3 Hz.

These observations demonstrate that the wave spectrum under typical, rather than carefully chosen, oceanic conditions is not solely determined by local winds but is the result of the temporal and spatial history of winds experienced by the waves. The observed spectra cannot be decomposed into a locally generated sea and a swell component propagating from remote sources; this may be a consequence of the meteorological regime particular to the Tropics.

1. Meteorology Department, Massachusetts Institute of Technology, Cambridge, Massachusetts, 02139, U.S.A.

2. University of California, San Diego, Scripps Institution of Oceanography, La Jolla, California, 92093, U.S.A.

## 1. Introduction

In recent years, observations of the spectrum of surface waves have been made in simple environments where the fetch, $x$, is well defined and the wind is uniform over the entire fetch and has been blowing steadily for a long duration. Under such conditions, empirical relations have been found (Hasselmann *et al.*, 1973) relating spectral parameters such as the frequency of the power spectrum peak, $f_m$, and the wave height variance, $\sigma^2$, to the nondimensional fetch $\tilde{x} = xg/U^2$ and the nondimensional frequency $\tilde{f} = 2\pi fU/g$ where $g$ is the gravitational acceleration and $U$ is the wind speed. Observations from a wide range of conditions are fairly well described by these relations, lying within a factor of 2 or 3 of the empirical curves.

These parameterizations, while important for a better understanding of the wave generation processes, are of uncertain utility when applied to the description of the wave spectrum under conditions more typical of the open ocean. The concepts of fetch and duration are quite nebulous there since the wind field is highly variable temporally and spatially and waves propagate tens of thousands of wavelengths with little energy dissipation (Snodgrass *et al.*, 1966). Under high winds of long duration, wave energy propagating from distant generation areas may be effectively masked by locally generated waves. In such a case, Pierson and Moskowitz (1964) propose an empirical form for the limiting power spectrum which is fetch-independent and has only the wind speed $U$ as a parameter.

$$P(f) = \alpha g^2 f^{-5} \exp\{-\beta(g/U)^4 f^{-4}\}$$

where $\alpha,\beta$ are constants. An even simpler limiting spectral form without dependence on the wind speed was proposed by Phillips (1958) who argued that at sufficiently high wind speeds the spectrum is limited by active wave breaking; the spectrum then has the universal form $P(f) = \gamma g^2 f^{-5}$ for frequencies $f$ greater than some cutoff frequency and where $\gamma$ is a universal constant. This simpler form is identified as the high frequency limit of the Pierson-Moskowitz spectrum.

The purpose of the experiment described here was to investigate both the power spectrum and the directional spectrum of oceanic surface waves on a day-to-day basis and to determine whether the observations may usually be described by any simple model. The applicability of the Pierson-Moskowitz spectrum and Phillips saturation spectrum to typical, rather than carefully screened, data was to be investigated as was the appropriateness of scalings based on local wind speed observations. Because of the difficulty of obtaining the quantity of data required, high resolution observations of directional spectra are few. Hence a second experimental objective was to obtain a representative description of the directional spectrum of open ocean waves and to examine this data for any clues it might provide concerning their dynamics.

## 2. The experiment

As part of the Barbados Oceanographic and Meteorological Experiment (BOM-

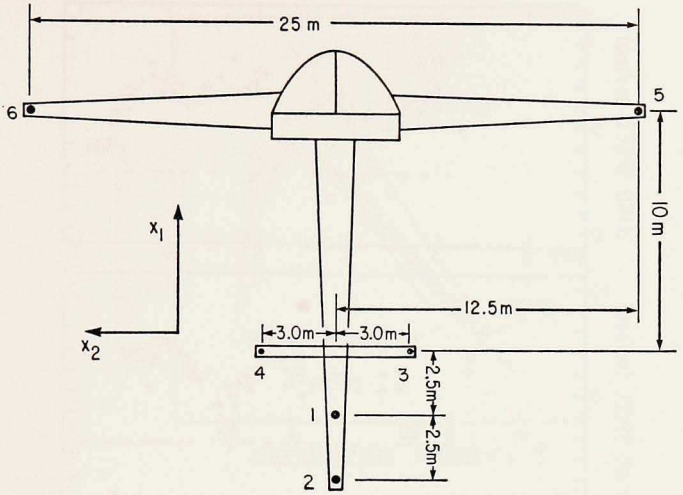


Figure 1. The array of sensors used to estimate the directional wave spectrum during BOMEX. A top view of FLIP and its booms is shown along with solid dots denoting the six elements of the array.

EX), the Research Platform FLIP was stationed about 300 km east of Barbados at latitude 15 degrees north during May of 1969. Wave height measurements were obtained from the array of wave sensors shown in Figure 1; measurements prior to 1500z hours of 13 May were obtained from the five sensors labeled 2, 3, 4, 5 and 6 in this figure and after that time all six elements were used. The wave sensors were of the resistance-wire type and consisted of Nichrome wire wrapped helically around a one inch diameter plastic pipe. The staffs were 5 meters long and had a resistivity of 110 ohms per meter. A 10 kgm weight was suspended 5 meters below the bottom of the pipe to maintain the sensor vertical with its midpoint near mean sea level. An AC resistance bridge excited by a 2 kilohertz square wave provided an output proportional to the resistance of the portion of the staff above water. This signal was recorded on analog magnetic tape over runs lasting up to six hours.

Analog tapes were digitized at a sampling rate of 4 Hz with a one part in 4096 resolution (a least-count error of a millimeter). The records were edited to remove dropouts of the recording system and instances where the wave amplitude exceeded the range of the wave staffs. After editing (which involved less than .05% of the data) the discrete Fourier transform of the output of each wave sensor was computed using a fast Fourier technique with an elementary bandwidth of .0039 Hz. The transformed wave records were corrected for the tilting motions of FLIP using a procedure described in Appendix F of Regier (1975). The correction is negligible for frequencies above .25 Hz but is unreliable below .08 Hz. Consequently the spectra below are restricted to frequencies above .08 Hz. The power spectrum of

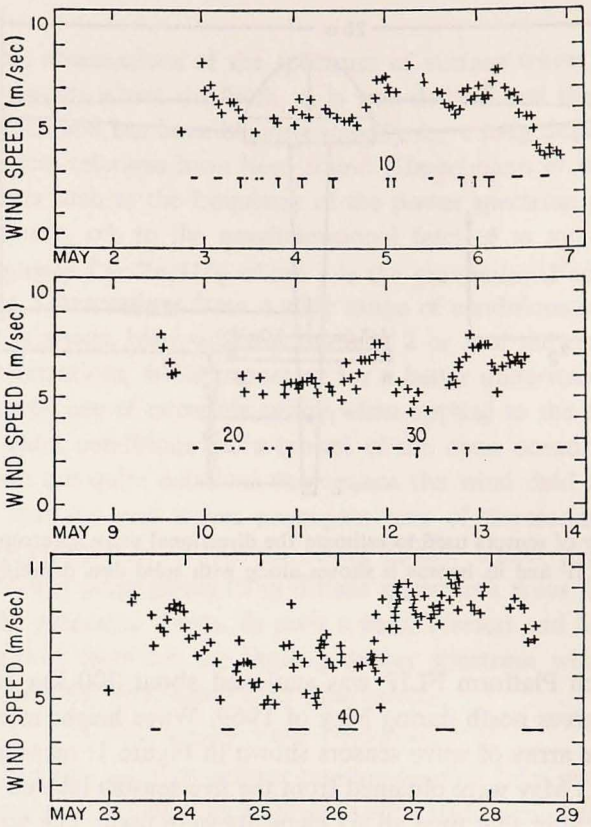


Figure 2. Wind speed observed on FLIP during BOMEX. Horizontal bars denote the extent of wave recording runs and the numerals indicate the run number. Those bars which form the top of a T are steady wind runs as defined in the text.

the corrected wave height is estimated to have less than 5% error for frequencies between .08 Hz and .13 Hz, and negligible error at higher frequencies.

Wind speed measurements were recorded by other experimenters on board FLIP. The wind speeds observed at an anemometer height of 11-12 meters above mean sea level are shown in Figure 2. The extent of the wave recording runs are shown as horizontal bars, indicating the length of the recording run. For 13 of the runs the wind speed deviated less than 1 $ms^{-1}$ from the mean value during the recording run and the preceding six hours; these steady wind runs are denoted in Figure 2. The wind speeds are seen to be quite variable and generally lower than is typically experienced in a trade winds region. Wind direction remained within 20 degrees of due east over the one month duration of the experiment.

No direct observations were made of the drift of the wave array. The drift of FLIP is estimated from daily fixes to be about .25 m $s^{-1}$ usually in the downwind

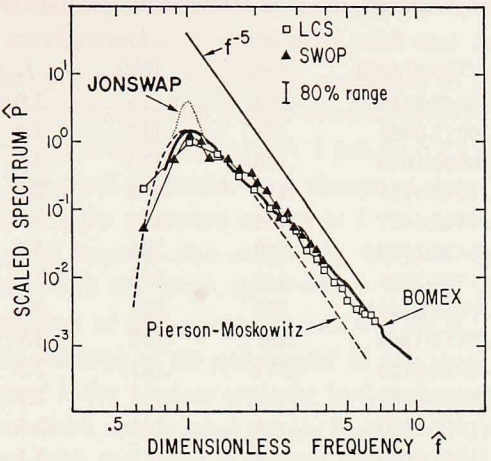


Figure 3. Scaled frequency power spectrum observed in BOMEX. See the text for definitions of the scaled spectrum $\hat{P}$ and the frequency parameter $\hat{f}$. Also shown are the Pierson-Moskowitz empirical spectrum, a line with slope proportional to $\hat{f}^{-5}$, the mean JONSWAP spectrum, the spectrum observed by Longuet-Higgins, Cartwright and Smith, and that observed during the Stereo Wave Observation Project. Only that portion of the JONSWAP spectrum significantly differing from the Pierson-Moskowitz model has been shown.

direction. Since the near surface water is presumably also moving downwind, the actual relative velocity between the array and the wave rest frame is probably somewhat less. Wavenumber frequency spectrum estimates of several BOMEX runs have been examined and show no clear departure from the theoretical dispersion relation due to array motion. On the basis of this and static balances of wind and water drag on FLIP it is not thought that the array velocity can exceed .1 m $s^{-1}$.

### 3. Observations of the power spectrum

The cross-spectra for each pair of elements was computed by averaging together the appropriate Fourier amplitude products for four minute data blocks in each run. A power spectrum was computed as the average of the autospectra for each run. The number of equivalent degrees of freedom of this estimate is at least 60 and more typically 200 if the individual elements are considered uncorrelated and 1/5 this if they are perfectly correlated. The spectrum averaged over all 42 runs is drawn as a heavy line in Figure 3. Following Mitsuyasu (1968), the frequency and spectrum are scaled by $f_m$, the frequency of the power spectrum peak, and $\sigma^2$, the variance of wave height, according to

$$\hat{P}(\hat{f}) = P(f) \cdot f_m/\sigma^2 \qquad \text{where } \hat{f} = f/f_m \qquad \text{and } \sigma^2 = \int_0^\infty P(f)\, df\,.$$

Table 1. Power spectrum parameters and wind observations.

| Run Number | Date/Time(local) | $\sigma^2$ ($m^2$) | $f_m$ (Hz) | $\hat{f}_b$ | $U$ (m $s^{-1}$) |
|---|---|---|---|---|---|
| 1 | 2/2047-2215 | .174 | .110 | 3.0 | — *n* |
| 2 | 3/0252-0437 | .171 | .117 | 2.9 | 7.0 |
| 3 | 3/0900-1030 | .176 | .110 | 3.0 | 6.0 *s* |
| 4 | 3/1045-1115 | .180 | .113 | 2.8 | — *n* |
| 5 | 3/1345-1427 | .161 | .117 | 3.7 | — *n* |
| 6 | 3/1430-1530 | .160 | .106 | 3.1 | — *n* |
| 7 | 3/1900-2000 | .148 | .113 | 3.5 | 5.2 *s* |
| 8 | 4/0045-0245 | .203 | .113 | 3.6 | 5.7 *s* |
| 9 | 4/0853-1100 | .167 | .110 | 3.9 | 5.9 *s* |
| 10 | 5/0020-0120 | .171 | .121 | 2.3 | 6.9 *s* |
| 11 | 5/0130-0225 | .174 | .121 | 2.3 | 7.0 *s* |
| 12 | 5/1115-1230 | .189 | .113 | 2.8 | — *n* |
| 13 | 5/1905-2040 | .152 | .117 | 3.1 | 6.1 *s* |
| 14 | 5/2310-2345 | .166 | .102 | 3.7 | 6.3 *s* |
| 15 | 6/0137-0428 | .174 | .110 | 2.8 | 6.6 *s* |
| 16 | 6/0915-1137 | .187 | .106 | 2.7 | 6.8 |
| 17 | 6/1640-1830 | .148 | .117 | 4.2 | 4.9 |
| 18 | 9/2120-2230 | .170 | .121 | 2.4 | — *n* |
| 19 | 10/0249-0512 | .193 | .133 | 2.0 | — *n* |
| 20 | 10/0725-0800 | .174 | .117 | 1.9 | — *n* |
| 21 | 10/0945-1042 | .134 | .125 | 2.3 | 6.0 |
| 22 | 10/1555-1633 | .142 | .149 | 3.4 | — *n* |
| 23 | 10/1742-1820 | .148 | .153 | 3.1 | — *n* |
| 24 | 10/2134-2247 | .128 | .129 | 2.9 | 5.4 *s* |
| 25 | 11/0850-0942 | .163 | .113 | 2.8 | 5.5 *s* |
| 26 | 11/1315-1352 | .170 | .117 | 3.7 | 5.6 |
| 27 | 11/1641-1801 | .193 | .125 | 3.2 | 5.9 |
| 28 | 11/2015-2212 | .228 | .129 | 3.0 | 6.6 |
| 29 | 12/0140-0400 | .204 | .133 | 2.8 | 6.7 |
| 30 | 12/0715-0815 | .178 | .121 | 3.3 | 5.1 *s* |
| 31 | 12/1725-1825 | .177 | .133 | 3.4 | 5.8 |
| 32 | 12/2024-2118 | .193 | .133 | 3.0 | 6.2 *s* |
| 33 | 12/2345-0614 | .215 | .125 | 2.6 | 6.9 |
| 34 | 13/0925-1053 | .256 | .125 | 2.5 | 6.5 |
| 35 | 13/1509-1647 | .272 | .110 | 2.7 | — *n* |
| 36 | 13/2044-2246 | .341 | .121 | 1.7 | — *n* |
| 37 | 23/1325-1545 | .581 | .102 | 2.4 | 8.7 |
| 38 | 24/1130-1507 | .496 | .102 | 2.6 | — *n* |
| 39 | 25/0829-1430 | .384 | .102 | 3.1 | 6.7 |
| 40 | 26/0000-0600 | .349 | .106 | 3.1 | — *n* |
| 41 | 27/0640-1233 | .408 | .106 | — *b* | 9.3 |
| 42 | 28/0942-1600 | .464 | .110 | 2.6 | 8.6 |
| LCS | | .25 | .095 | 2.9 | 10.0 |
| SWOP | | .12 | .122 | 2.0 | 9.5 |

*b* no bend in the spectrum.
*n* no wind observations during run.
*s* steady winds during run and six preceding hours.

The vertical error bar indicates that 80% of the estimates lie within ± 40% of the mean value. Other nondimensionalizations were tried and resulted in far greater amounts of scatter; in particular, $\hat{f} = 2\pi fU/g$, equivalent to the ratio of wind speed to wave phase speed, was found to be a poor nondimensional frequency parameter.

The mean spectrum has a maximum at $\hat{f} = 1$ followed by a rapid decay with increasing frequency. The mean spectrum has a change of slope, or bend, at $\hat{f} = \hat{f}_b \approx 3$; at frequencies below $\hat{f}_b$ the spectrum decays as $\hat{f}^{-3.1}$ and is proportional to $\hat{f}^{-4.3}$ above $\hat{f}_b$. The change of slope is also evident in the individual spectra that were averaged together to obtain the mean spectrum. A quartic polynomial was least-squares fit to the logarithm of each spectrum over the range $\hat{f} > 1$ and the point of maximum rate of slope change of the polynomial fit was used to identify $\hat{f}_b$ for that spectrum. The values of $\hat{f}_b$ for 41 runs (one run had no bend) lay in the range from 1.6 to 4.2; the 13 runs with steady wind speeds had $2.3 \leqslant \hat{f}_b \leqslant 3.9$. The BOMEX spectra are consistent with the wave pole data obtained during the Stereo Wave Observation Project (SWOP) by Chase *et al.* (1957) and the pitch-roll buoy observations of Longuet-Higgins, Cartwright and Smith (1963) (hereafter referred to as LCS) both with regard to overall dependence on frequency and to the existence of a discernible $2 < \hat{f}_b < 3$. The values of $\sigma^2$, $f_m$, $\hat{f}_b$, and $U$ for the BOMEX, LCS, and SWOP data are tabulated in Table 1. The mean JONSWAP (Joint North Sea Wave Project) spectrum, observed by Hasselmann *et al.* (1973) during development at fetches up to 160 km, is of a substantially different shape.

None of the spectra exhibit the $f^{-5}$ dependence of the theoretical Phillips saturation spectrum, possibly because the wind speeds were rather low and never exceeded 10 m s$^{-1}$. The Pierson-Moskowitz spectrum model is based on a carefully chosen set of observations with wind speeds greater than 10 m s$^{-1}$. Although this parameterization is a good fit to those observations, Moskowitz (1964) reports little success in describing randomly chosen data. Thus it is not surprising that the BOMEX, SWOP, and LCS spectra do not agree with the Pierson-Moskowitz model. Figure 4, a plot of observed $\sigma^2$ versus $f_m$, demonstrates that these important spectral parameters differ greatly from the predictions of the Pierson-Moskowitz model; the large scatter evident in this plot further suggests that no single-parameter model of the power spectrum is adequate and that at least two parameters are required to model the spectrum of oceanic waves. Hasselmann *et al.* (1976) conclude that the spectrum of waves developing in a limited fetch is well determined by a single parameter; in view of Figure 4, extending this conclusion to a description of the development of the spectrum in the open sea would seem unwise.

For all of the BOMEX observations, the phase speed corresponding to the frequency $f_m$ is roughly twice the local wind speed $U$. The phase speed of waves at the bend in the spectrum is slightly less than $U$ as may be seen in Figure 5. The correlation coefficient of $U$ with $P(\hat{f}_b)$ is .806, indicating $U$ and $P(\hat{f}_b)$ are correlated at the 99% significance level. The correlation coefficients of $U$ and $P(\hat{f})$ shown in

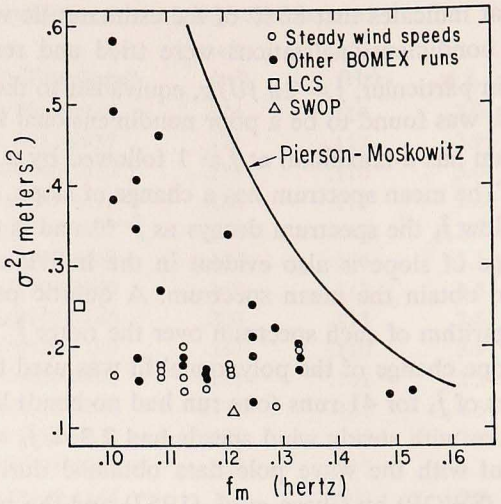


Figure 4. The relation between wave variance, $\sigma^2$, and the frequency of the peak of the power spectrum. The considerable scatter suggsts single parameter model spectra cannot well describe trade-wind sea states.

Table 2. Correlation of spectral density $P(\hat{f})$ with wind speed. Significance levels less than 50% are indicated by a dash(—).

| $\hat{f}$ | Correlation Coefficient | Level of Significance |
|---|---|---|
| .5 | .50 | 90% |
| 1.0 | −.12 | — |
| 1.5 | −.03 | — |
| 2.0 | .64 | 99% |
| 2.5 | .46 | 95% |
| 3.0 | .37 | 90% |
| 3.5 | .34 | 80% |
| 4.0 | .15 | 50% |
| 4.5 | .11 | — |
| 5.0 | .19 | 50% |
| 5.5 | .11 | — |
| 6.0 | .03 | — |
| 6.5 | .01 | — |
| 7.0 | .07 | — |
| 7.5 | .04 | — |
| 8.0 | −.10 | — |
| 8.5 | −.06 | — |
| 9.0 | −.18 | 50% |
| 9.5 | −.11 | — |
| 10.0 | −.11 | — |

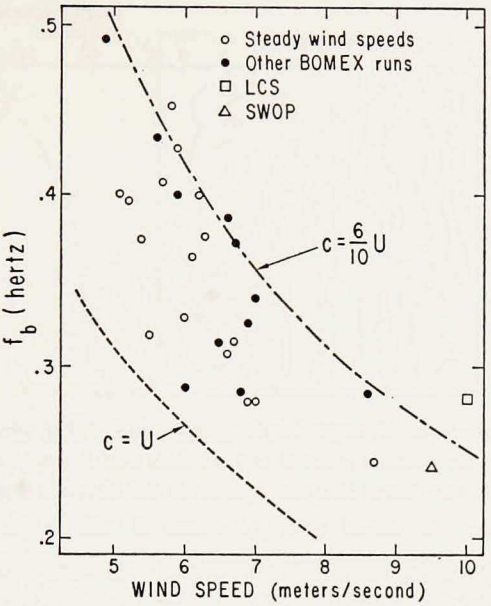


Figure 5. The relation between the wind speed and $f_b$, the frequency separating the two power spectral slopes.

Table 2 reveal a correlation at the 80% level for frequencies around $\hat{f}_b$ in the range $2 < \hat{f} < 3.5$. On this basis it might be surmised that the transfer of energy from the wind to the waves occurs primarily in the region of the bend in the spectrum. However, this must remain conjecture until direct measurements are available of the nonlinear transfer of energy within the spectrum. Hasselmann *et al.* (1973) have predicted this transfer on theoretical grounds and find that the input of wind energy to the mean JONSWAP spectrum occurs at frequencies between $f_m$ and $3f_m$; however, the difference in shape between the BOMEX and JONSWAP spectra may greatly alter the nature of the nonlinear transfer function. The band of negative correlation between wind speed and spectral levels for frequencies above $\hat{f} = 8$ is interesting, but the significance level is less than 50%.

## 4. Observations of the directional spectrum

Various methods of estimating the directional spectrum of waves from array data have been described and compared by Davis and Regier (1977). The conclusion of that study was that, over a broad range of conditions, the Data Adaptive Spectral Estimator (DASE) produced more accurate spectral estimates than any other of the data adaptive or *a priori* optimized methods tested. The reader is referred to this study and Regier (1975) for a description of the method and an assessment of its performance.

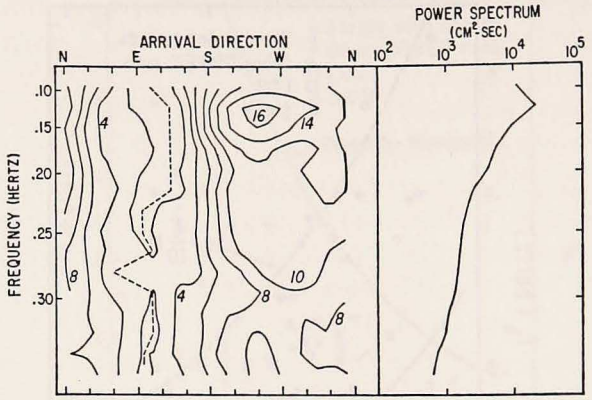


Figure 6. The power spectrum, $P$, and directional spectrum, $S(\theta;f)$, observed during run 9. In the contour plot of $S$ the contour interval is 2 decibels and the contours are labeled as decibels down from $S = 1$. The dotted line corresponds to the directional peak.

The directional spectrum estimate is obtained from the matrix of cross-spectra of all element pairs in the array. The cross-spectra were computed as described in §3 and then averaged with respect to frequency over a bandwidth inversely proportional to frequency; this results in bands with constant wavenumber widths, $\Delta k$. For a wave of wavenumber $k$, the phase lag between sensors separated by distance

Table 3. Frequency bands of the directional spectrum estimates.

| Center Frequency (Hertz) | Bandwidth (Hertz) | Wavelength (meters) |
|---|---|---|
| .094 | .031 | 176.6 |
| .125 | .024 | 99.8 |
| .151 | .020 | 68.4 |
| .174 | .020 | 51.5 |
| .196 | .016 | 40.6 |
| .215 | .016 | 33.7 |
| .233 | .012 | 28.7 |
| .248 | .012 | 25.4 |
| .264 | .012 | 22.4 |
| .280 | .012 | 19.9 |
| .295 | .012 | 17.9 |
| .311 | .012 | 16.1 |
| .325 | .008 | 14.8 |
| .336 | .008 | 13.8 |
| .348 | .008 | 12.9 |
| .360 | .008 | 12.0 |
| .371 | .008 | 11.3 |
| .383 | .008 | 10.6 |

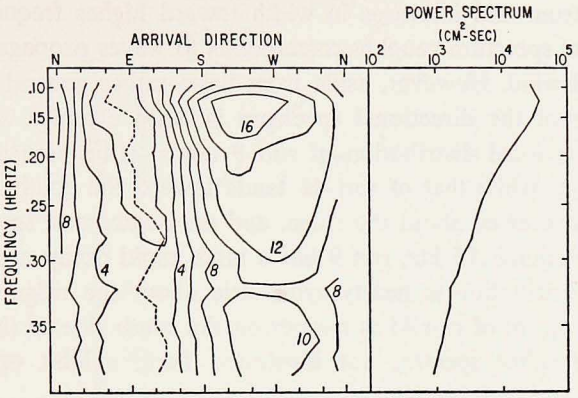


Figure 7. As Figure 6 for run 41.

$\rho$ is of the order $\phi \approx k\rho$ so that in averaging over bands of constant width $\Delta k$, the range of phase angles averaged together is roughly the same for all bands. The center frequencies of the bands for which cross-spectra and directional spectra were computed are shown in Table 3; the wavenumber width of the bands is approximately .024 $m^{-1}$. A typical BOMEX data run allowed 20 estimates of the cross-spectrum for each element pair and each frequency. The band-averaged cross-spectra were averaged over at least 40 independent values (the highest frequency band contains two Fourier components). Thus the expected standard deviation of the directional spectrum estimate is approximately 16% of the average of the estimate; this corresponds to .7 db on a logarithmic scale.

Regier (1975) has presented contour maps of all 42 power and directional spectral estimates made from the BOMEX data. These are too numerous to show here. Contour maps of the directional spectra for runs 9 and 41 are shown in Figures 6 and 7. The contour interval is in 2 db and the directional spectrum $S(\theta;f)$ has been normalized so $\int_{-\pi}^{\pi} S(\theta;f)d\theta = 1$ for each frequency band. Spectral estimates were computed at 12 degree intervals using the DASE algorithm. The dashed line indicates the ridge or crest of the angular distribution at each frequency. The five-element array consisting of sensor 2, 3, 4, 5, and 6 (see Fig. 1) was used on run 9 and the full six-element array was used during run 41. The five-element array is spatially aliased at wavelengths shorter than 12 meters which restricts frequencies to less than .36 Hz; the six-element array is usable up to .5 Hz. The expected sample variability of the spectrum estimate of run 9 is .5 db while that of run 41 is .3 db.

The gross features of these spectra and others obtained during BOMEX and by other workers are quite similar. The angular distribution is narrow near the peak of

the power spectrum and increases in width toward higher frequencies. The ridge of the directional spectrum roughly corresponds to waves propagating in the direction of the local wind. However, aside from these rather general observations, the actual character of the directional spectrum is quite complex and variable. The ridge of the directional distribution of run 9 tends to become more northerly at higher frequencies while that of run 41 tends toward the south. The angular distribution is often skewed about the ridge, and the degree and sense of skewness is quite variable. Around .15 Hz, run 9 has a more rapid decay on the south side of the ridge; the distribution is nearly symmetric about the ridge above .3 Hz. In contrast, the spectrum of run 41 is steeper on the south side of the peak at all frequencies. Many other spectra, not illustrated here, exhibit opposite senses of skewness at low and high frequencies.

Several models of the directional spectrum were fit directly to the observed cross spectra. The parameters of each model $\hat{S}(\theta;f)$ were chosen to minimize the square error $E^2$

$$E^2 = \sum_{j=1}^{N} \sum_{l=j+1}^{N} |\hat{C}(\rho_{jl}; f) - C_{jl}(f)|^2$$

where

$$\hat{C}(\rho_{jl};f) = \int_{-\pi}^{\pi} \hat{S}(\theta;f) \exp\{i\, k(f)\, \rho_{jl} \cos(\theta - \phi_{jl})\} d\theta$$

is the predicted cross-spectrum at lag $\rho_{jl}$ obtained from the reverse transform of the model spectrum and $C_{jl}(f)$ is the observed cross-spectrum. One model spectrum was the cosine-power model used by LCS and Tyler *et al.* (1974) (later referred to as TTSPMJ)

$$\hat{S}(\theta;f) = A \cos^r(\xi/2), \qquad \xi = \theta - \theta_0 \tag{1}$$

where $A$ is chosen so $\int_{-\pi}^{\pi} \hat{S}(\theta;f)d\theta = 1$ and $r$ and $\theta_0$ are the model parameters. As might be expected, the observations were fit with less error by a skewed model

$$\hat{S}(\theta;f) = A \cos^{0.1}(\xi/2) \cdot \begin{Bmatrix} \exp[-\mu\, \xi^2], & 0 < \xi \leqslant \pi \\ \exp[-\nu\, \xi^2], & -\pi < \xi \leqslant 0 \end{Bmatrix} \tag{2}$$

where $A$ is as above and $\theta_0, \mu$, and $\nu$ are the parameters of the model; the $\cos^{0.1}(\xi/2)$ factor assures continuity of the model at $\xi = -\pi$. For both models the minimization of $E^2$ was accomplished by a gradient-search method and required extensive amounts of computer time since $E^2$ was found to have several local minima. For this reason it was economically feasible to fit only the data of runs 9 and 41 to models.

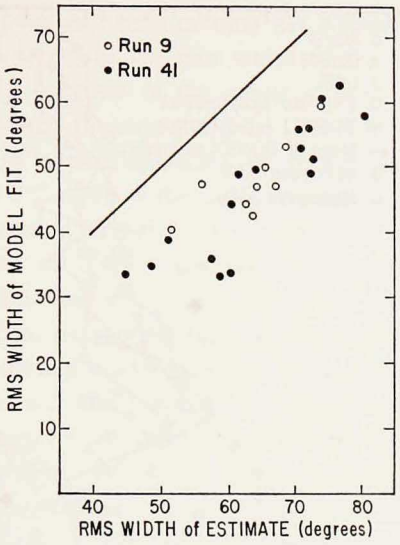


Figure 8. The *RMS* directional spectrum width, $\theta_{rms}$, as determined directly from the estimated spectrum and by fitting the observed cross-spectra to those for the skewed model spectrum as defined in the text. The discrepancy appears to result from the inability of a simple model spectrum to describe actual directional spectra.

The width of an angular distribution $S(\theta;f)$ may be conveniently expressed by

$$\theta^2_{rms} = \int_{\theta_m-\pi}^{\theta_m+\pi} (\theta-\theta_m)^2 S(\theta;f)d\theta$$

where $\theta_m$, the mean angle of the distribution, is the solution to the integral equation

$$0 = \int_{\theta_m-\pi}^{\theta_m+\pi} (\theta-\theta_m)S(\theta;f)d\theta\,.$$

The root-mean-square (*rms*) width of the skewed model fits and spectrum estimates of runs 9 and 41 are plotted against each other in Figure 8. Only observations for frequencies greater than 0.094 Hz and less than 0.28 Hz are shown. Lower frequency waves are too long to be adequately resolved by the array and higher frequency waves, with wavelengths comparable to the minimum array separations, are aliased.

The spectrum estimate widths and the widths of the model fits are highly correlated, increasing and decreasing together, but the widths of the spectral estimates are 15 to 20 degrees greater. A test of the spectrum estimator on simulated data having an angular distribution proportional to $\cos^4(\theta/2)$ revealed the *rms* width of the spectrum estimate to be 57 degrees, only 6 degrees greater than the actual width of 51 degrees. Thus the large discrepancy between the widths of the model

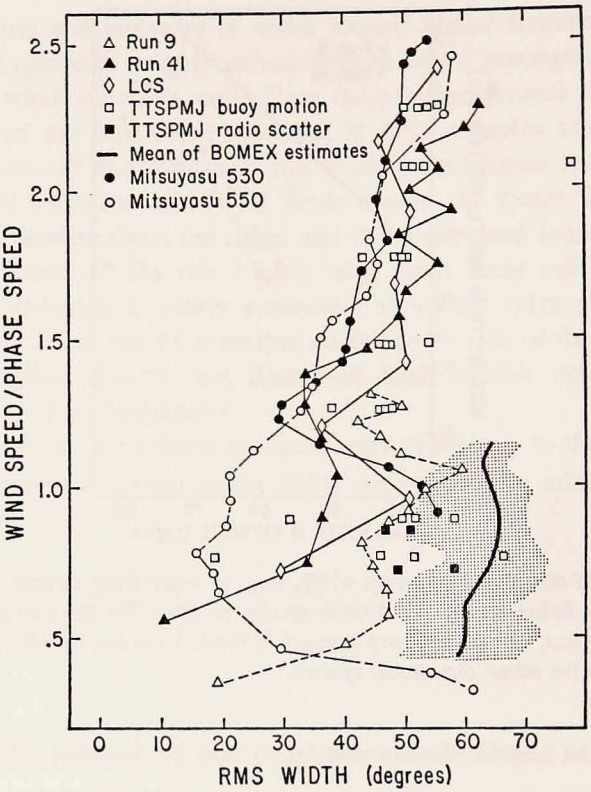


Figure 9. *RMS* width of the directional wave spectrum as a function of $U/c$. The symbols for BOMEX runs 9 and 41 are obtained from fits to the skewed model described in the text. The solid curve represents the mean width obtained directly from the BOMEX estimated directional spectra and the shaded area is the range of widths. Also shown are the results obtained by Mitsuyasu and by Longuet-Higgins, Cartwright and Smith, both obtained from fits to models of the form $\cos^r(\theta/2)$. The highest resolution observations are probably those by Tyler *et al.* for which the widths are computed without use of a model.

fits and the spectrum estimates is not thought to be due to limited resolution of the array.

A source of discrepancy between angular widths computed from model fits and from spectral estimates is the inability of the model to represent the form of the actual spectrum. While both the cosine-power and skewed models appear to be flexible, both have the weakness that the model behavior near the peak cannot be specified independently of the behavior at large angular distances from the maximum. It is to be expected that the process of fitting a model to observed cross-spectra attempts to minimize the error of the fit where most of the energy is concentrated, i.e., near the peak of the directional spectrum. In this case the behavior of the model at great distances from the peak is completely specified by the nature

of the spectrum near its peak and may or may not resemble the actual spectrum. This may lead to serious errors in the rms width of the model, the width being particularly sensitive to the behavior of the model at large displacements from $\theta_m$.

A simulation was performed to determined the sensitivity of estimates of spectral width to Doppler shifting of wave frequencies due to a downwind drift of the array. It was found that a .5 m $s^{-1}$ drift of the array is sufficient to broaden the actual spectrum width by 30 degrees. However, the importance of this effect cannot be accurately assessed because no direct measurements of the downwind drift of the array are available. As discussed in §2, we estimate the array drift to be less than .1 m $s^{-1}$ which is too small to account for the discrepancies in spectral width.

The rms widths of the skewed model fits to the data of runs 9 and 41 are plotted versus the ratio of wind speed, $U$, to wave phase speed, $c$, in Figure 9. The mean width of the spectrum estimates for the 13 steady wind speed runs is drawn as a heavy line, and the range of values is indicated by the shaded area. For values of $U/c$ exceeding 1.2 the model widths are fairly consistent with observations made with pitch-roll buoys by LCS, TTSPMJ, and Mitsuyasu *et al.* (1975) and suggest that the width of the directional spectrum increases as $U/c$ increases. At $U/c$ ratios less than 1.2, the trend is ill-defined but appears to have the same sense.

The spectra observed by TTSPMJ using radio scatter techniques have widths intermediate between the buoy observations and the spectrum estimates obtained during BOMEX. As the radio observations have a resolving ability of about ± 3 degrees, they are regarded as giving the most reliable estimates of spectral width. The buoy data of LCS, TTSPMJ, and Mitsuyasu have been analyzed by fitting cosine-power models of the form of (1) to the cross-spectra between the observed buoy motions. This procedure is relatively simple as the cross-spectra are trigonometric moments of the directional spectrum and should result in reliable estimates of the spectral width if the spectrum indeed has a form consistent with a cosine-power model. Several values of $r$, the exponent of the fit, may be obtained from each buoy observation and all the values of $r$ should be identical if the cosine-model is correct. In fact, the values are observed to disagree, often substantially, indicating that the assumed cosine-power model of the spectrum is not correct. The buoy used by Mitsuyasu also measures the curvature of the sea surface thus giving higher order moments of the spectrum which are quite sensitive to the actual spectral form; he attributes the large deviations between the values of $r$ obtained from these moments and those obtained from the lower order moments to inaccurate curvature measurements rather than a failure of the cosine-power model; to us the latter seems more likely, but the nature of the bias introduced into the spectral width estimates by deviation of the actual spectrum from the assumed model form is not clearly known. It does appear that the spectral width may be rather poorly estimated from buoy data if the actual spectrum disagrees significantly with the cosine model.

Table 4. Correlation coefficient of rms angular width of the spectrum estimate with wind speed.

| Frequency (Hertz) | Correlation Coefficient |
|---|---|
| .125 | −.256 |
| .151 | −.572 |
| .174 | −.265 |
| .196 | −.413 |
| .215 | −.520 |
| .233 | −.447 |
| .248 | −.735 |
| .264 | −.582 |

| Confidence Level | Correlation Coefficient |
|---|---|
| 50% | .206 |
| 80% | .380 |
| 90% | .476 |
| 95% | .684 |
| 99% | .801 |

The correlation coefficient of wind speed and the *rms* width of the spectrum estimates for the 13 steady wind speed runs is tabulated in Table 4 as a function of frequency. Since Figure 8 shows the model widths and estimate widths to be highly correlated for the available range of frequencies, this table also reflects the correlation of the model widths with wind speed. The correlation is seen to be consistently negative with the level of significance at least 50% and usually greater than 80%. This implies that at a fixed frequency (or fixed wave phase speed) the spectral width decreases as $U$ increases. This apparently contradicts the tendency for spectral widths to increase with increasing $U/c$ when that parameter is less than 1.2, and suggests the inadequacy of this scaling for low frequencies. No data are available to similarly check the validity of the wind speed scaling at values of $U/c$ greater than 1.2.

In Figure 10 the data of Figure 9 are plotted versus $\hat{f}$, the ratio of frequency to the frequency of the power spectrum peak; the degree of scatter is roughly the same in the two plots. In view of the opposite trends of width against $U$ and $U/c$, it would appear more reasonable to describe the directional width of the spectrum in terms of $\hat{f}$ than the more conventional wind speed scaling, at least for waves with $U/c < 1.2$. It is interesting to note that the tendency for $\theta_{rms}$ to increase with $\hat{f}$ appears to be interrupted by a narrowing of the spectrum near $\hat{f} = 2$ and, to a lesser degree, near $\hat{f} = 3$; this feature is not clearly defined and is not evident in the width of the spectral estimates themselves.

## 5. Conclusions

This experiment has shown that the spectrum of oceanic surface waves is only

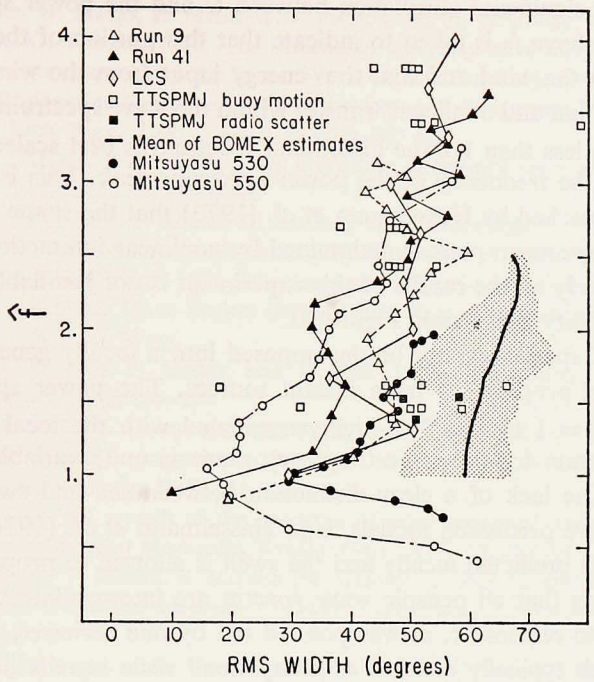


Figure 10. *RMS* width of the directional wave spectrum as a function of $\hat{f} = f/f_m$. See the caption of Figure 9 for symbol definitions.

poorly described by simple models. The observed power spectra are not consistent with the theoretical Phillips saturation model or the empirical Pierson-Moskowitz model. The lack of a reliable relation between wave height variance and the frequency of the power spectrum peak implies that at least two parameters are required to model adequately the oceanic power spectrum and that single-parameter models, such as the Pierson-Moskowitz model, are inadequate to describe typical power spectra. The variability in the skewness and width of the directional spectra indicates that waves propagating from distant generation areas are important in determining spectral properties. They also raise serious questions with regard to the practice of fitting observations to simple models derived from prescribed directional spectra.

Scaling frequencies by the ratio of wind speed to wave phase speed does not coalesce the observed power spectra and leads to an inconsistency in the description of the width of the directional spectrum at frequencies between $f_m$ and $f_b$.

The angular width of the directional spectrum is determined quite well by $U/c$, the ratio of wind speed to wave phase speed, when $U/c$ exceeds 1.2. This frequency range roughly corresponds to waves having frequencies near and above $f_b$, the frequency of the bend in the power spectrum, for which $U/c$ ranges from 1 to 1.6.

The lack of any significant correlation between $U$ and the power spectrum density for frequencies above $f_b$ is taken to indicate that this portion of the spectrum is in equilibrium with the wind and that the energy input from the wind is nearly balanced by dissipation and nonlinear transfer within the wave spectrum.

At $U/c$ ratios less than 1.2 the directional spectrum is best scaled by $\hat{f}$, the ratio of frequency to the frequency of the power spectrum peak. This is consistent with the conclusion reached by Hasselmann *et al.* (1973) that the shape of the spectrum near the power spectrum peak is maintained by nonlinear interactions. Such a conclusion based solely on the results of this experiment is not justifiable in view of the significant variability apparent in Figure 10.

The BOMEX spectra cannot be decomposed into a locally generated sea and a swell component propagating from distant sources. The power spectrum for frequencies from $\hat{f} = 1$ to $\hat{f} = 3$ is highly correlated with the local wind while the directional spectrum for the same frequency range is quite variable, indicating remote sources. The lack of a clear distinction between sea and swell may present problems for wave prediction models, e.g., Hasselmann *et al.* (1976), in which the sea component is predicted locally and the swell is allowed to propagate. However, before concluding that all oceanic wave spectra are intermediate between sea and swell, it is well to remember, as was pointed out by one reviewer, that the tropical wind field, which typically consists of many small scale squalls distributed quasi-randomly in space and time, is quite unlike the higher latitude wind regime where high wind speeds are concentrated in a few large scale storms. Thus one might expect the directional spectrum to be more isotropic and to exhibit a greater degree of variability in the Tropics than at higher latitudes; we are unaware of any observations which can be compared with the BOMEX spectra to examine this hypothesis. It is interesting to note, however, that the LCS and SWOP power spectra, both observed near 40°N, are similar in shape and frequency dependence to the tropical BOMEX observations.

As the wind speeds were rather low during this experiment, and in light of the discussion above, it is perhaps inadvisable to extend these conclusions to spectra under higher wind speeds and outside the Tropics. It is clear that high resolution estimates of the spectrum and direct measurements of the nonlinear transfer of wave energy are required under high winds to further explore the questions raised by this study. However, the observed features of change in spectral slope at $f_b$ and correlations relating directional spread to both wind speed and $f_m$ may provide some simple tests of theoretical models.

## REFERENCES

Barber, N. F. 1963. The directional resolving power of an array of wave detectors, *in* Ocean Wave Spectra, Englewood Cliffs, N.J., Prentice-Hall, 137–150.

Capon, J. 1969. High-resolution frequency-wavenumber spectrum analysis, Proc. IEEE, *57*, 1408–1418.

Chase, J., L. J. Cote, W. Marks, E. Mehr, W. J. Pierson, Jr., F. G. Ronne, G. Stephenson, R. C. Vetter, and R. G. Walden. 1957. The directional spectrum of a wind generated sea as determined from data obtained by the Stereo Wave Observation Project, New York University, College of Engineering Department of Meteorology and Oceanography and Engineering Statistics Group, Tech. Rept. ONR Contract 285(03), 267 pp.

Davis, R. E., and L. Regier. 1977. Methods for estimating directional wave spectra from multi-element arrays, J. Mar. Res., *35,* this issue.

Hasselmann, K., T. P. Barnett, E. Bouws, H. Carlson, D. E. Cartwright, K. Enke, J. A. Ewing, H. Gienapp, D. E. Hasselmann, P. Kruseman, A. Meerburg, P. Müller, D. J. Olbers, K. Richter, W. Sell, and H. Walden. 1973. Measurements of wind-wave growth and swell decay during the Joint North Sea Wave Project (JONSWAP), Erganzungsheft zur Deut. Hydrogr. Zeitschrift, Reihe A(8°), *12,* 95 pp.

Hasselmann, K., D. B. Ross, P. Müller, and W. Sell. 1976. A parametric wave prediction model, J. Phys. Oceanogr., *6,* 200–228.

Longuet-Higgins, M. S., D. E. Cartwright, and N. D. Smith. 1963. Observations of the directional spectrum of sea waves using the motions of a floating buoy, *in* Ocean Wave Spectra, Englewood Cliffs, N.J., Prentice-Hall, 111–136.

Mitsuyasu, H. 1968. On the growth of the spectrum of wind-generated waves (I), Reports of Research Institute for Applied Mechanics, Kyushu Univ., XVI, *55,* 459–482.

Mitsuyasu, H., F. Tasai, T. Suhara, S. Mizuno ,M. Ohkusu, T. Honda, and K. Rikiishi. 1975. Observations of the directional spectrum of ocean waves using a cloverleaf buoy, J. Phys. Oceanogr., *5,* 750–760.

Moskowitz, L. 1964. Estimates of the power spectrums for fully developed seas for wind speeds of 20 to 40 knots, J. Geophys. Res., *69,* 5161–5179.

Phillips, O. M. 1958. The equilibrium range in the spectrum of wind-generated waves, J. Fluid Mech., *4,* 426–434.

Pierson, W. J., Jr., and L. Moskowitz. 1964. A proposed spectral form for fully developed wind seas based on the similarity theory of S. A. Kitaigorodskii, J. Geophys. Res., *69,* 5181–5190.

Regier, L. 1975. Observations of the power and directional spectrum of oceanic surface waves, Ph.D. dissertation, Univ. of Calif., San Diego.

Snodgrass, F. E., G. Groves, K. Hasselmann, G. Miller, W. Munk, and W. Powers. 1966. Propagation of ocean swell across the Pacific, Phil. Trans. Roy. Soc. London, Series A, *259,* 431–497.

Tyler, G., C. Teague, R. Stewart, A. Peterson, W. Munk, and J. Joy. 1974. Wave directional spectra from synthetic aperture observations of radio scatter, Deep-Sea Res., *21,* 989–1016.

Received: *3 September, 1976;* revised: *28 February, 1977.*